

See discussions, stats, and author profiles for this publication at: <https://www.researchgate.net/publication/331712276>

Estimating the Effect of Rotor Diameter on the Physical Properties of NACA0015 Airfoil-Based Vertical-Axis Wind Turbine

Article in *Journal of Physics Conference Series* - February 2019

DOI: 10.1088/1742-6596/1178/1/012003

CITATIONS

0

READS

5

2 authors:



Raid Khider Salman
University of Anbar

8 PUBLICATIONS 1 CITATION

[SEE PROFILE](#)



Waleed Bdaiwi
University of Anbar

33 PUBLICATIONS 10 CITATIONS

[SEE PROFILE](#)

Some of the authors of this publication are also working on these related projects:



Modeling of MEMS device [View project](#)



Material science [View project](#)

PAPER • OPEN ACCESS

Estimating the Effect of Rotor Diameter on the Physical Properties of NACA0015 Airfoil-Based Vertical-Axis Wind Turbine

To cite this article: Raid Khider Salman and Waleed Bdaiwi 2019 *J. Phys.: Conf. Ser.* **1178** 012003

View the [article online](#) for updates and enhancements.



IOP | ebooks™

Bringing you innovative digital publishing with leading voices to create your essential collection of books in STEM research.

Start exploring the [collection](#) - download the first chapter of every title for free.

Estimating the Effect of Rotor Diameter on the Physical Properties of NACA0015 Airfoil-Based Vertical-Axis Wind Turbine

Raid Khider Salman, Waleed Bdaiwi

College of Education for Pure Science, University of Anbar

Author E-mail: dr.raid1978@hotmail.com

Abstract. This study combines aerodynamic and structural analyses on a vertical-axis wind turbine (VAWT) built using NACA0015 airfoil-based blades. Aerodynamic analyses consist of velocity and pressure profiles as well as the drag behaviour. Structural investigations have included stress and displacement of the blade to the airflow pressure. This study has highlighted the effect of the diameter variation on VAWT physical performance. The results have showed a positive effect of the rotor diameter on the laminar flow and Von Karman vortex street. The drag coefficient behaviour was reduced with the diameter increase due to the reduction of the wake within the thin layers of the laminar behind the streamlined airfoils. Also, the structural stress and displacement were negatively affected by the diameter increase.

1. Introduction

NACA airfoils are novel airfoils structures that have been invented and developed by the National Advisory Committee for Aeronautics (NACA)[1, 2]. The four-digit NACA refers to an airfoil that can be characterized by four design parameters. Mainly, there are two types of 4-digit NACA; the symmetrical 4-digit NACA and the cambered 4-digit NACA. The reason behind this classification is to optimise the aerodynamic characteristics of the main structure either for the aircraft wings or for the wind turbine blades. Each number after the “NACA” word refers to one of the design parameters. For example, NACA 2412 foil represents an airfoil of a maximum camber of 0.2 of its chord length and a distance of 0.4 from it. The last two digits 12 indicate that the maximum thickness is 0.12 (12%) of the chord length. The symmetrical 4-digit NACA airfoil is normally characterized by the term NACA 00xx, where 00 indicates no camber for this NACA (i.e. the camber line coincide with the axis of symmetry) and the xx represents the ratio of thickness to the chord length[3, 4]. The current study uses the symmetrical 4-digit NACA airfoil since it is used commonly in wind turbine blade design.

A symmetrical NACA can be characterized by four major parameters that can control its design as shown in Figure 1. These are; c- Chord length ; t_{max} - maximum thickness ; r- Leading edge radius ; ξ - Trailing edge angle.

The equation by which 4-digit symmetrical NACA airfoil can be designed and built can be given by [1, 2]

$$y_t = 5t[0.2969\sqrt{x} - 0.1260x - 0.3516x^2 + 0.2843x^3 - 0.1015x^4] \quad (1)$$

The independent variable x represents the horizontal location along the chord which ranges from 0 to 1. y_t represents a function of it's the chord points.

The position where which the NACA airfoil reaches its maximum thickness along the chord can be found by applying the first derivative in Equation 1 above. Which yields;



$$\pm y'_t = 5t \left[\frac{0.14845}{\sqrt{x}} - 0.126 - 0.7032x + 0.8529x^2 - 0.406x^3 \right] \quad (2)$$

And find the value of x at $y'_t=0$. Which gives $x_{\text{max}} = 0.2998278781$ of the chord length (C).
Leading edge radius is proportional with the square of thickness as follows;

$$r = 1.1019t^2 \quad (3)$$

The trailing edge angle can be calculated interms of $y'_t(1)$ (the first dervative of y_t at $x=1$), i.e.;

$$\tan \xi = y'_t(1) = -1.16925t \quad (4)$$

Although NACA was developed for the aircraft wing in the first place, its design principle has been exploited to produce high-efficiency wind turbine blades[7]. The virtue of employing NACA airfoil in wind turbine blades building is the ease of aerodynamics controlling, predicting and hence mathematically optimising before the real-time use.

Vertical-axis wind turbines (VAWT) have several advantages over the horizontal wind turbine (HAWT), regarding the volume-power efficiency, urban setting possibilities as well as the ease in fixing and domestic productivity, as well as working with lower wind speed. Nevertheless, merging NACA-blades within the VAWT structures need much care and extensive aerodynamic investigations before building. The favourable attitude of VAWT construction seems the direct practical approach, which cannot be in parallel with the best performance and efficiency. The best approach yet to achieve these tasks is the computer modelling and simulation, which offers many accurate and reliable calculations, as well as time and effort saving. However, few studies have included using NACA-blades in VAWT within this methodology. The modelling tools for design and investigate NACA airfoils were used since the 1930s, but the developing of CAD systems and computer programming and hardware has expanded the design and investigation processes. Claessens has submitted a good relative study using two written-codes named RFOIL and VAWT simulation program. The first one was used to calculate the properties of 2D airfoils, meanwhile, the second one (VAWT) was used to estimate the VAWT performance using the 2D airfoil results [8]. Another good article has dealt with the studying of the aerodynamics of small VAWT using overset grid method [9]. In which, the authors have studied the possibility of using NACA 0015 airfoil to build a VAWT for low wind speed (5 m/s) by the aid of computational fluid dynamics (CFD). The variables which have been included in this study are power coefficients and tip speed ratios (TSRs) $\lambda=2-7$ as well as the dynamic stall effect. They have concluded that the best power coefficient (0.45) can be attained at $\lambda=4$ and λ has a negative effect on the dynamic stall. Carrigan et.al. have introduced a fully automated CAD system for aerodynamic shape optimization applied to VAWTs which have showed a promising performance in relating with the structure development and maximizing its efficiency[10]. Another good 2d numerical investigations for a VAWT-based wind farm has been suggested by Durrani et al. [11]. They have investigated the effect of wake vortices from one VAWT to another in the clustering area. Other studies have included structural investigations and the suitable materials for wind turbine blades [12-15]. Most of the nominated articles have used either aerodynamic behaviour for the wind turbine or only structural studies. Moreover, the aerodynamic studies concentrate only on the lift behaviour; nevertheless, the drag force is also a big factor in the aerodynamic outline.

The present study investigates the effect of the VAWT diameter on its structural and aerodynamic behaviour. It is devoted to answer a big question which is "how likely the VAWT diameter can affect its performance especially the wake effect and the VAWT stiffness?" The aerodynamic part of the study includes the velocity and pressure profiles as well as the consequent drag. The structural part of the study includes the response of the blade to the airflow pressure which is represented by the blade maximum displacement and the structural stress. The major aim of all these investigations is to show the suitability

of NACA- based VAWT design for the low wind speed areas such as the Middle East regions and specifically in Iraq.

2. Design and analyses processes

Autodesk Inventor Professional has been used to design the mainframe structure of the VAWT; meanwhile, the aerodynamic profiles have been investigated by Autodesk Flow Design Software using the computational fluid dynamics CFD method. The modelling methods NACA 0015 airfoil- based blades have been designed within the same environment and then emerged into the VAWT mainframe.

Figure 2 shows the design of NACA0015 and its distribution along the VAWT propeller.

The mainframe with the airfoil blades is illustrated in Figure 3.

Unplasticised polyvinyl chloride (PVC) has been used as a blade material, which its properties are illustrated in Table 1

. The resulting VAWT was 1m height. Wind speed in simulation has been chosen to meet the up-to-date weathercast data of the city of Ramadi, west of Baghdad/Iraq (latitude:33.4336, longitude:43.3057). The weather parameters have been collected using “Windfinder” webpage <https://www.windfinder.com/#10/33.4412/43.3026>. According to this website, on wind speed recorded on Tuesday 7th of August 2018, was 4.63m/s (9kts).

3. Results and Discussion

3.1. Aerodynamic Analyses

Figure 4 shows the aerodynamic velocity patterns of the air passing the NACA 0015 airfoils within different rotor diameters.

All the graphs show a steady and ordered air flow through the airfoils (the air flows from the left side), with a weak turbulence far behind the smooth surfaces. Despite this weak turbulence, it causes a significant drag that is highly affected by the rotor diameter as illustrated in Figure 5.

Since the drag coefficient (C_d) is inversely proportional with the projected area A (the product of thickness and length of the blade) according to the relationship; (Where F_d is the drag force, ρ is the air density and U_{mean} is the mean velocity).

$$C_d = \frac{2F_d}{\rho U_{mean}^2 A} \quad (5)$$

It is supposed to have a progressively decrease in the drag amount with the increase in the VAWT diameter (including the blade distance from the VAWT axis).

However, in Figure 6 the drag coefficient develops aperiodic variation accorded with Von Karman vortex variation as shown in the velocity graphs above. Furthermore, as the diameter increases up to 900mm, the drag exhibit non-uniform variation showing a noisy curve, which starts retrieve its periodicity at $1100\text{mm} \leq D < 1500$. Similar periodicity has been reported by Carrigan et. al. [10], who revealed that such periodicity is also an indication for the torque variation with the main work parameters. Brusca et. al. [19] attributed this behaviour to the variation of the angle of attack with the diameter variation, which in turn affects Reynolds number.

The velocity contour plots show more uniform Von Karman Vortex Street streams. At low diameters ($D \leq 1100\text{mm}$) the vortices of each airfoil interfere with the others. This behaviour is no longer detected at high diameters (normally at $D \geq 1400\text{mm}$). The maximum vortex result from the airfoil that faces the

airflow, meanwhile the other two have fewer vortices due to the maximum angle of attack that the first one makes with the airflow in comparison with the others. No significant effect has been observed from the airflow on the local speed of the airfoil.

Figure 6 demonstrates the evolution of the airflow pressure around the airfoils. As can be seen, the pressure varies periodically with the increase in rotor diameter showing minimum values at $D=1000\text{mm}$ and $D=1100\text{mm}$.

3.2. Structural analyses

Structural analyses have been accomplished after the aerodynamic analyses; since the aerodynamic pressure which has resulted from the airflow pressure is required to be used as a structural load applied on the VAWT NACA 0015 blades. The pressure load has been applied normally to the blade surface with the aid of the following equation[19];

$$\nabla \cdot P = \mu \nabla \cdot (\nabla u + (\nabla u)^T) - \frac{2}{3} \cdot \mu (\nabla \cdot u) - \rho \cdot (u \cdot \nabla) \cdot u \quad (6)$$

Where ρ the density of the fluid (air), p the pressure (Pa), u is the displacement response of the model to the applied pressure, and μ is the fluid viscosity. The structural analyses have been solved by Stress Analysis add-in related to the finite element method.

With a minimised value of 9Pa (as result from the pressure profile). Figure 7 illustrates the blade response to the aerodynamic pressure load for one of the structural case studies.

The maximum stress seems to be directly proportional to the displacement on one hand, but inversely with the diameter on the other hand as shown in Figure 8 and Figure 9.

However, the stress shows a good agreement to somehow with the drag coefficient behaviour except at some points in the middle. Both stress and the drag coefficient behaviour exhibit fluctuated curves and participate with a top value at $D=700\text{mm}$, which is 0.047MPa for stress and 1.037 for the drag coefficient behaviour. Two other distinctive peaks can be detected within the C_d curve, corresponding to the diameters 1100mm and 1400mm, which are 1.011 and 0.958.

4. Conclusions

Aerodynamic and structural studies on NACA0015-based VAWT have been made with a standard speed of wind matching the western area of Iraq specifically in Ramadi. The results have showed a clear improvement in laminar flow with the increase in the rotor diameter. Von Karman Vortex Street has been refined significantly when the diameter becomes wider. This refining in the vortex has reduced the wake behind the streamlined objects and hence has reduced drag coefficient behaviour. No noticeable increase in pressure has been identified. Structural properties showed a gradual dropping with the diameter increase.

References

- [1] Aeronautics, U.S.N.A.C.f., NACA technical note1958.
- [2] Aeronautics, U.S.N.A.C.f., NACA RM1956: National Advisory Committee for Aeronautics.
- [3] Sheldahl, R.E. and P.C. Klimas, Aerodynamic characteristics of seven symmetrical airfoil sections through 180-degree angle of attack for use in aerodynamic analysis of vertical axis wind turbines, 1981, Sandia National Labs., Albuquerque, NM (USA).
- [4] Ahmed, M.R. and S. Sharma, An investigation on the aerodynamics of a symmetrical airfoil in ground effect. *Experimental Thermal and Fluid Science*, 2005. 29(6): p. 633-647.
- [5] Moran, J., *An Introduction to Theoretical and Computational Aerodynamics*2003: Dover Publications.

- [6] Ladson, C.L. and L.R. Center, Computer program to obtain ordinates for NACA airfoils 1996: National Aeronautics and Space Administration, Langley Research Center.
- [7] Adaramola, M., *Wind Turbine Technology: Principles and Design* 2014: CRC Press.
- [8] Claessens, M., *The design and testing of airfoils for application in small vertical axis wind turbines*. Master of Science Thesis, 2006. 9.
- [9] Bangga, G., et al. Aerodynamic performance of a small vertical axis wind turbine using an overset grid method. in *AIP Conference Proceedings*. 2017. AIP Publishing.
- [10] Carrigan, T.J., et al., Aerodynamic shape optimization of a vertical-axis wind turbine using differential evolution. *ISRN Renewable Energy*, 2012.
- [11] Durrani, N., et al. 2-D Numerical Analysis of a VAWT Wind Farm for Different Configurations. in *49th AIAA Aerospace Sciences Meeting including the New Horizons Forum and Aerospace Exposition*. 2011.
- [12] Babu, K.S., et al. The material selection for typical wind turbine blades using a MADM approach & analysis of blades. in *Proceedings of 18th International Conference on Multiple Criteria Decision Making (MCDM 2006)*, Chania, Greece, June. 2006.
- [13] Brøndsted, P., H. Lilholt, and A. Lystrup, Composite materials for wind power turbine blades. *Annu. Rev. Mater. Res.*, 2005. 35: p. 505-538.
- [14] Lachenal, X., S. Daynes, and P.M. Weaver, Review of morphing concepts and materials for wind turbine blade applications. *Wind energy*, 2013. 16(2): p. 283-307.
- [15] Veers, P.S., et al., Trends in the design, manufacture and evaluation of wind turbine blades. *Wind Energy: An International Journal for Progress and Applications in Wind Power Conversion Technology*, 2003. 6(3): p. 245-259.
- [16] Whelan, T. and J. Goff, *Unplasticised Polyvinyl Chloride*, in *Injection Molding of Thermoplastic Materials - 21990*, Springer US: Boston, MA. p. 142-155.
- [17] Titow, W.V., *PVC Plastics: Properties, Processing, and Applications* 2012: Springer Netherlands.
- [18] Brusca, S., R. Lanzafame, and M. Messina, Design of a vertical-axis wind turbine: how the aspect ratio affects the turbine's performance. *International Journal of Energy and Environmental Engineering*, 2014. 5(4): p. 333-340.
- [19] Ramana M. Pidaparti, M.B., Rebecca L. Heise, Angela Reynolds, Analysis for stress environment in the alveolar sac model. *Biomedical Science and Engineering*, 2013. 6: p. 901-907.

General	Mass Density	1.29 g/cm ³
	Yield Strength	40 MPa
	Ultimate Tensile Strength	40 MPa
Stress	Young's Modulus	709 MPa
	Poisson's Ratio	0.41
	Shear Modulus	251 MPa

Table 1 Unplasticised polyvinyl chloride properties[3, 4]

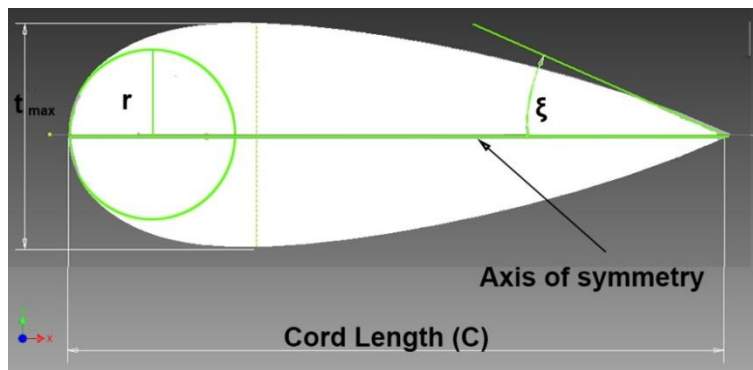


Figure 1 Symmetrical 4-digit NACA with its design parameters

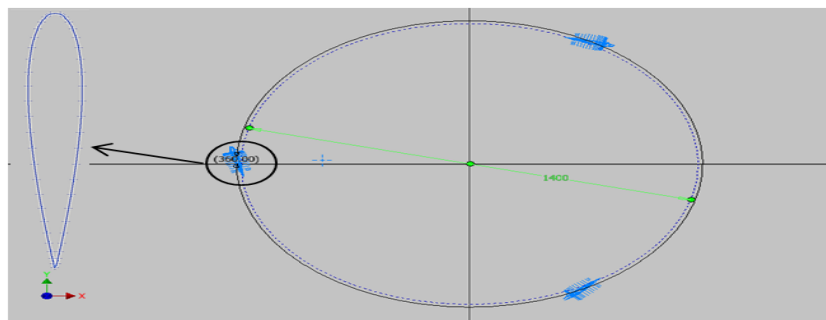


Figure 2 NACA 0015 design and distribution along the VAWT propeller path

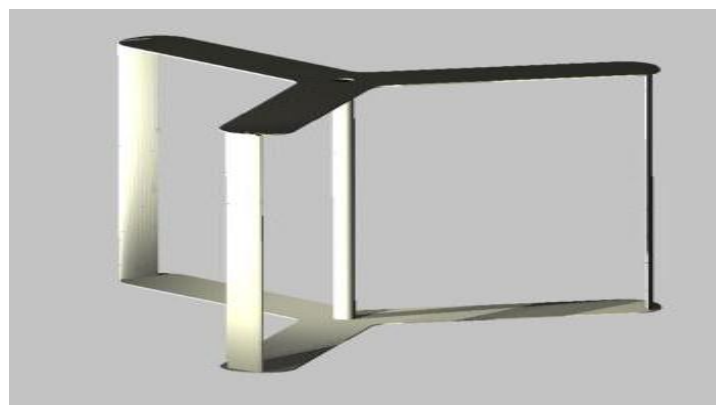


Figure 3 VAWT mainframe with the NACA0015 blades included

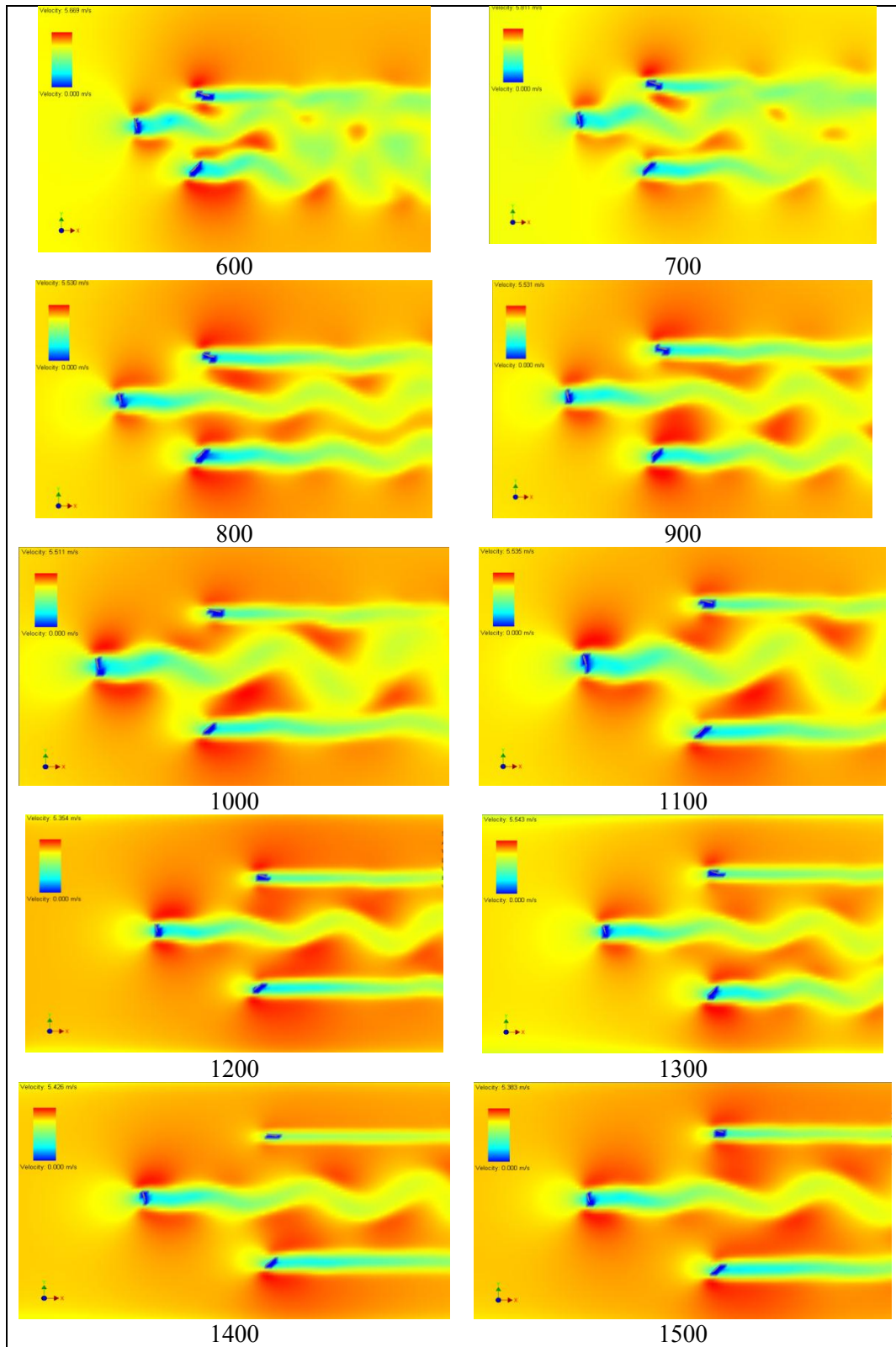


Figure 4 Airflow Velocity Profile for different VAWT diameters.

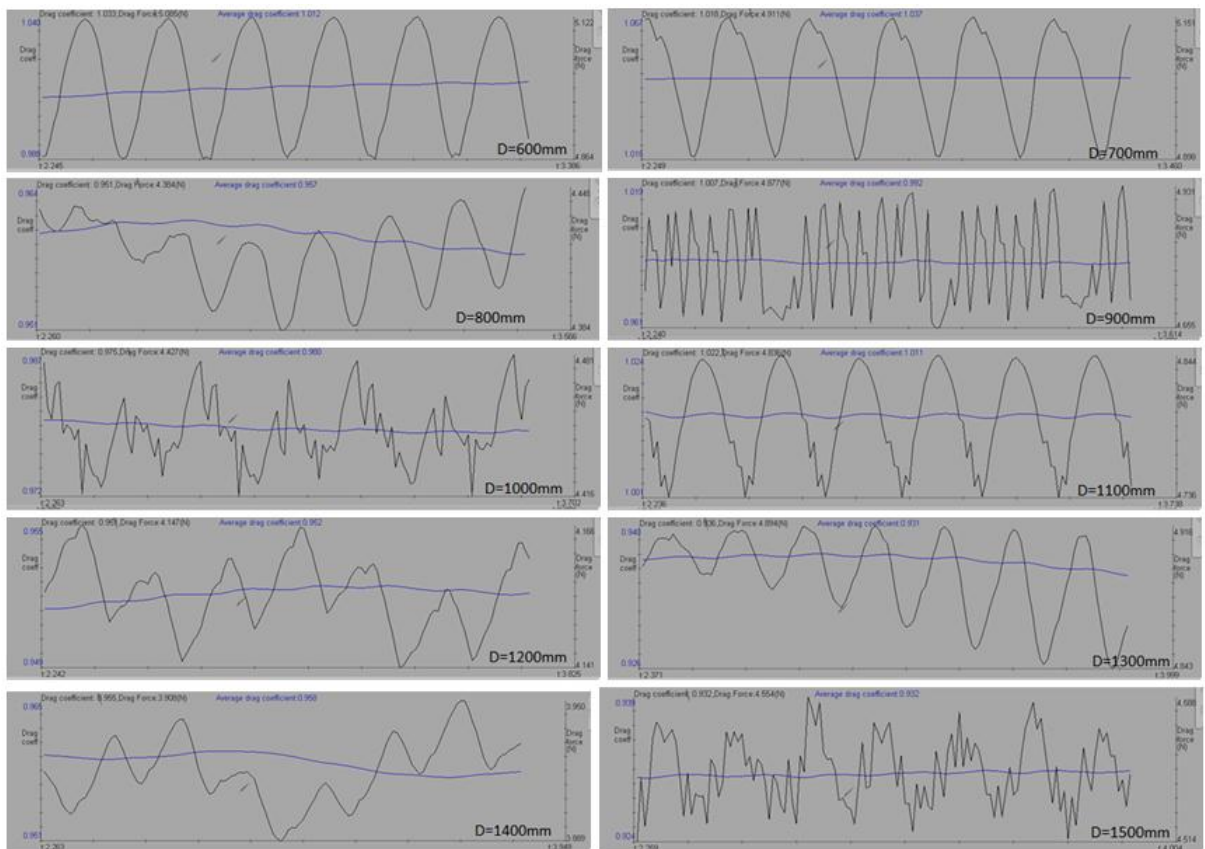
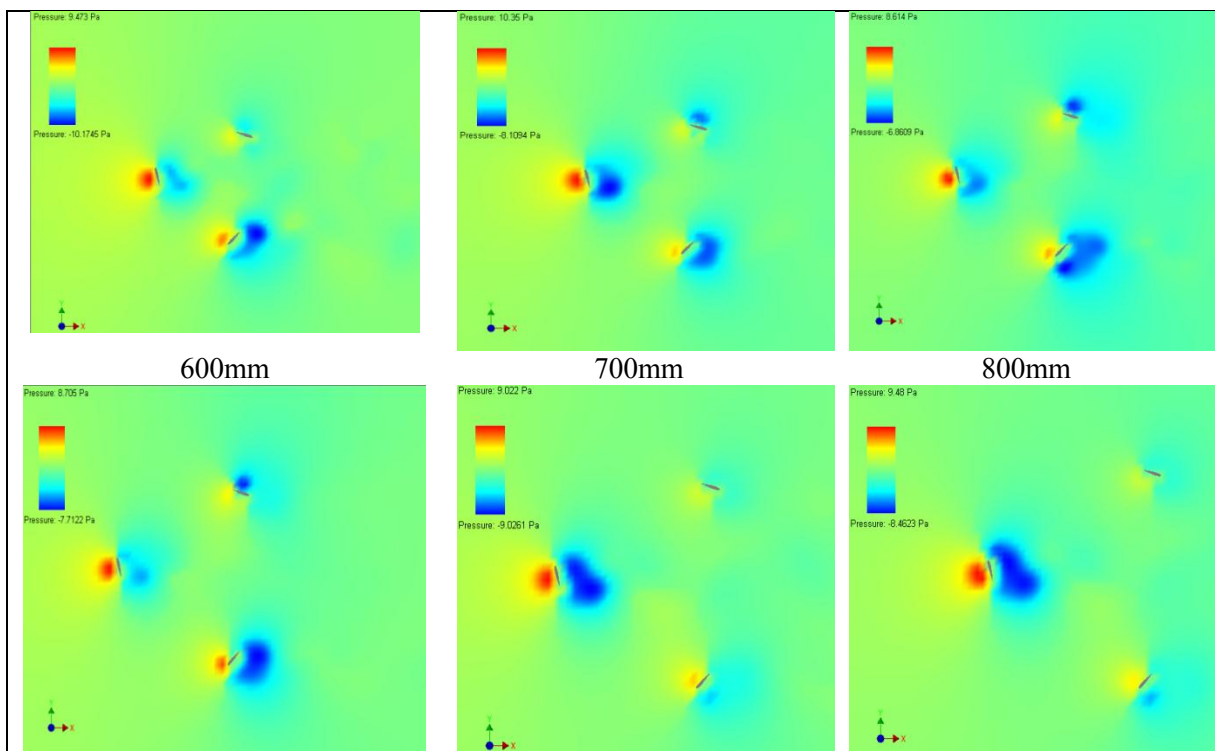


Figure 5 Drag plots for the VAWT airfoils at different diameters



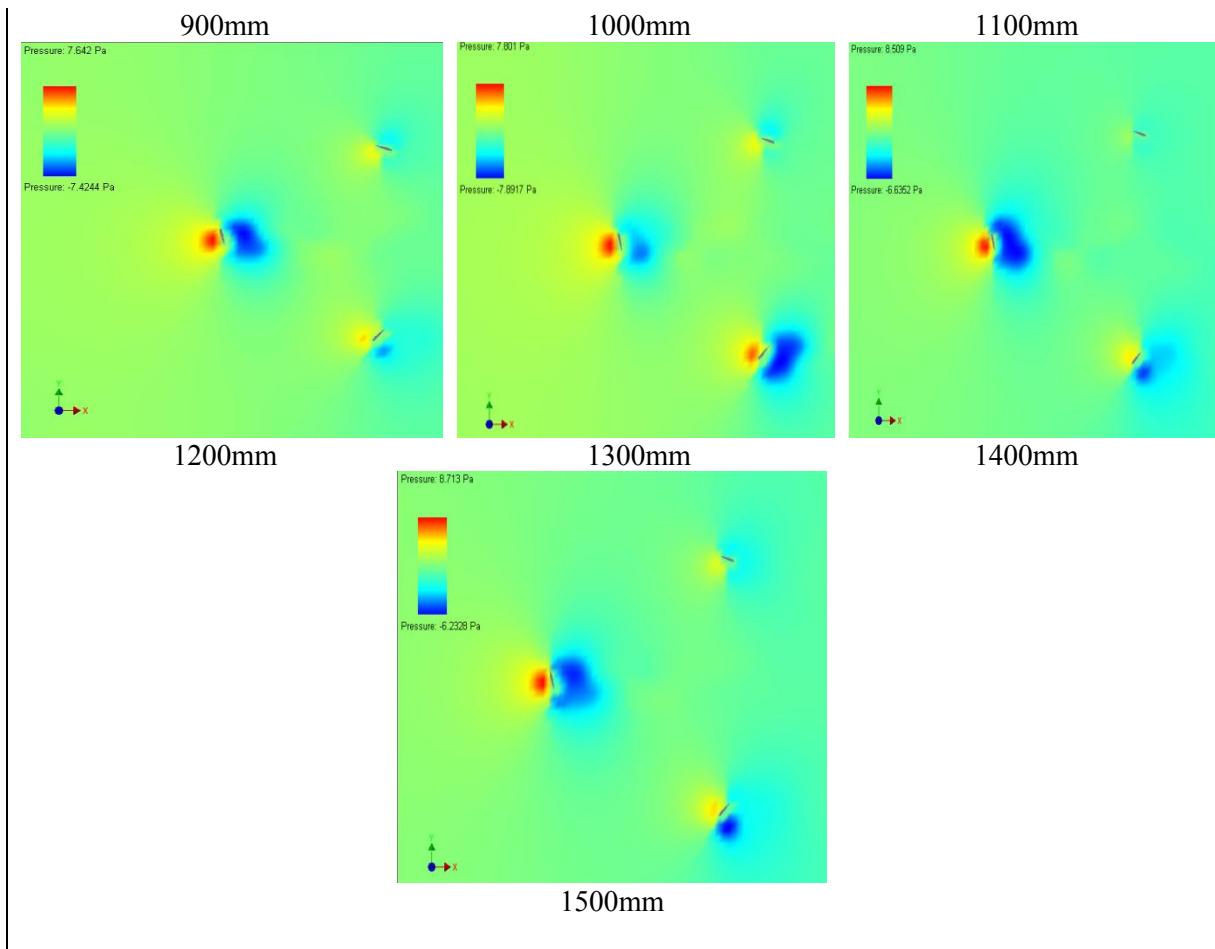


Figure 6 Aerodynamic pressure profile for the NACA 0015-based blades

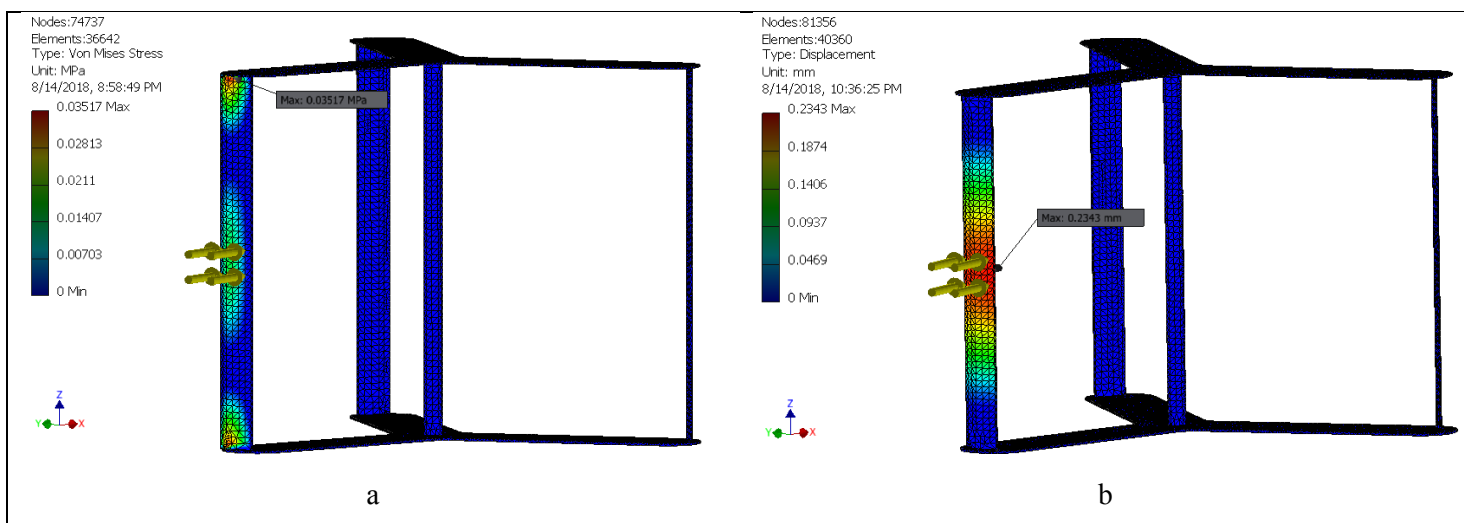


Figure 7 The response of the VAWT blade due to the airflow pressure; (a) Von Mises Stress (MPa) and (b) The displacement

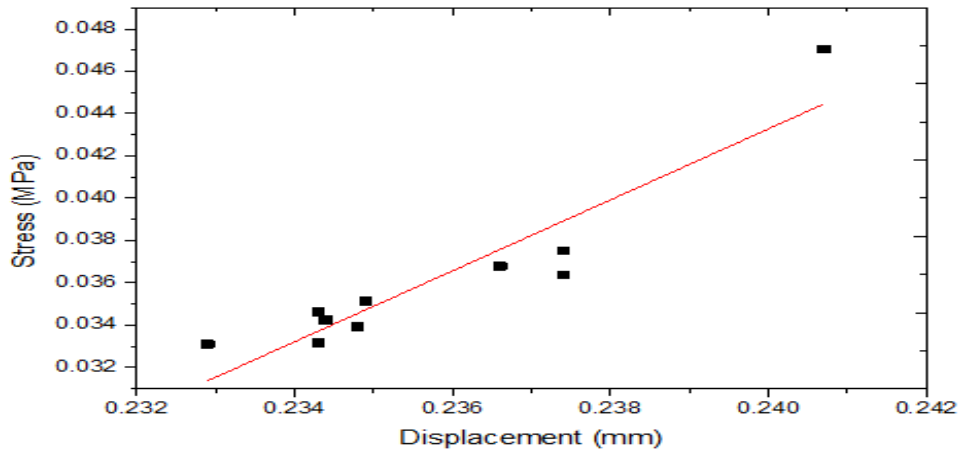


Figure 8 Stress- displacement curve.

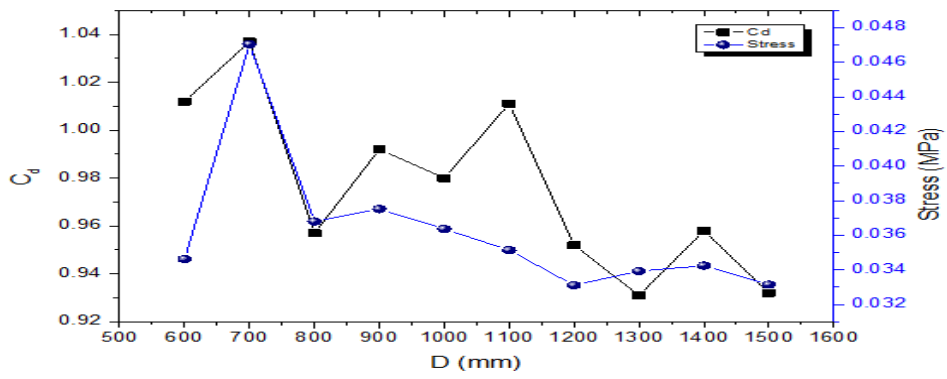


Figure 9 Drag Coefficient and Stress as a function of rotor diameter